Received: 2 March 2022 | Revised: 16 May 2022 | Accepted: 21 May 2022

DOI: 10.1002/ar.25011

SPECIAL ISSUE ARTICLE

The Anatomical Record | WILEY

New frontiers in imaging, anatomy, and mechanics of crocodylian jaw muscles

Casey M. Holliday[1] | **Kaleb C. Sellers**[1] | **Emily J. Lessner**[1] | **Kevin M. Middleton**[1] | **Corrine Cranor**[2] | **Conner D. Verhulst**[1] | **Stephan Lautenschlager**[3] | **Kenneth Bader**[4] | **Matthew A. Brown**[4] | **Matthew W. Colbert**[5]

[1]Department of Pathology and Anatomical Sciences, University of Missouri, Columbia, Missouri, USA

[2]Department of Geology and Geologic Engineering, South Dakota School of Mines and Technology, Rapid City, South Dakota, USA

[3]School of Geography, Earth and Environmental Sciences, University of Birmingham, Birmingham, UK

[4]Texas Vertebrate Paleontology Collection, Jackson School of Geosciences, University of Texas at Austin, Austin, Texas, USA

[5]Jackson School of Geosciences, University of Texas at Austin, Austin, Texas, USA

Correspondence
Casey M. Holliday, Department of Pathology and Anatomical Sciences, University of Missouri, Columbia, Missouri 65211, USA.
Email: hollidayca@health.missouri.edu

Present address
Kaleb C. Sellers, Clinical Anatomy and Osteopathic Principles and Practice, Rocky Vista University, Parker, CO, USA

Conner D. Verhulst, University of Missouri-Kansas City School of Medicine, Kansas City, Missouri, USA

Funding information
Missouri Research Board; National Science Foundation, Grant/Award Numbers: NSF DBI 1902242, NSF EAR 1631684, NSF EAR 1762458, NSF IOS 1457319; University of Missouri Research Council

Abstract

New imaging and biomechanical approaches have heralded a renaissance in our understanding of crocodylian anatomy. Here, we review a series of approaches in the preparation, imaging, and functional analysis of the jaw muscles of crocodylians. Iodine-contrast microCT approaches are enabling new insights into the anatomy of muscles, nerves, and other soft tissues of embryonic as well as adult specimens of alligators. These imaging data and other muscle modeling methods offer increased accuracy of muscle sizes and attachments without destructive methods like dissection. 3D modeling approaches and imaging data together now enable us to see and reconstruct 3D muscle architecture which then allows us to estimate 3D muscle resultants, but also measurements of pennation in ways not seen before. These methods have already revealed new information on the ontogeny, diversity, and function of jaw muscles and the heads of alligators and other crocodylians. Such approaches will lead to enhanced and accurate analyses of form, function, and evolution of crocodylians, their fossil ancestors and vertebrates in general.

KEYWORDS
crocodylia, microCT, jaw muscles, biomechanics, 3D modeling

1 | INTRODUCTION

Living crocodylians, and their extinct crocodyliform ancestors, catch the imagination of scientists and the public alike with their unique heads, armored and agile bodies and voracious feeding bouts. Recently, great strides have been made in understanding the functional morphology of the feeding apparatus of crocodylians including studies of anatomy (Bona and Desojo 2011; Bailleul and Holliday, 2017; Sellers et al., 2019; Kuzmin et al. 2021; Morris et al., 2021; Sellers, 2021), function (McHenry et al., 2006; Porro et al., 2013; Sellers et al.,

2017; Sellers et al., 2022), performance (Erickson et al., 2003; Kerfoot et al., 2014) and evolution (Melstrom and Irmis, 2019; Drumheller and Wilberg, 2019; Carr et al., 2021). Despite a reasonable understanding of the anatomy of the jaw muscles and their related soft tissues within the adductor chamber (e.g., Iordansky 1964; Schumacher 1973; Holliday and Witmer 2007, Porro et al., 2011; Tsai and Holliday 2011; Lessner and Holliday 2020), challenges interpreting their ontogeny, function, and evolution remain.

During crocodylomorph evolution, the suturing of the palate to the braincase not only brought about a secondary bony palate but also a set of jaw muscles seemingly less differentiated than those found in other diapsids such as lizards and birds. Muscles of the palate are typically easy to identify relative to the muscles of the braincase in other diapsids such as lepidosaurs and dinosaurs because of clear fascial planes and physical separation of bony muscle attachments among the surfaces of the braincase and palatoquadrate. In contrast, among crocodylians this muscle tissue is challenging to dissect in a consistent fashion and has fostered discussions of homology of muscles viz-a-viz the dorsotemporal fossa (Iordansky 1964; Schumacher 1973; Holliday and Witmer 2007,2009, Holliday and Gardner 2012; Bona et al., 2012; Holliday et al., 2019), braincase wall (Klembara 2004; Holliday and Witmer 2009), and trigeminal nerve divisions (Holliday and Witmer 2007; Lessner 2020). New contrast imaging approaches have proven effective at clarifying these details as well as revealing astounding anatomical details of extant crocodylians ranging from embryos to adults (Holliday et al., 2013; George and Holliday 2013; Gignac and Kley 2014; Gignac et al., 2016; Tsai and Holliday 2016; Lessner and Holliday 2020; Figures 1-5). Finally, these new anatomical approaches enable more refined 3D biomechanical approaches to understanding the function of the crocodylian skull where data from musculature can inform how the bones and joints of the skull are loaded during feeding behaviors (Sellers et al., 2017; Gignac and Erickson 2016).

Here, we share our experiences with new advances in the imaging and modeling of extant crocodylian heads with a focus on the jaw musculature, its functional morphology, and neighboring structures. We discuss contrast stained microCT of specimens including large fresh cadaveric specimens (Figures 2, 3), embryos (Figure 4),

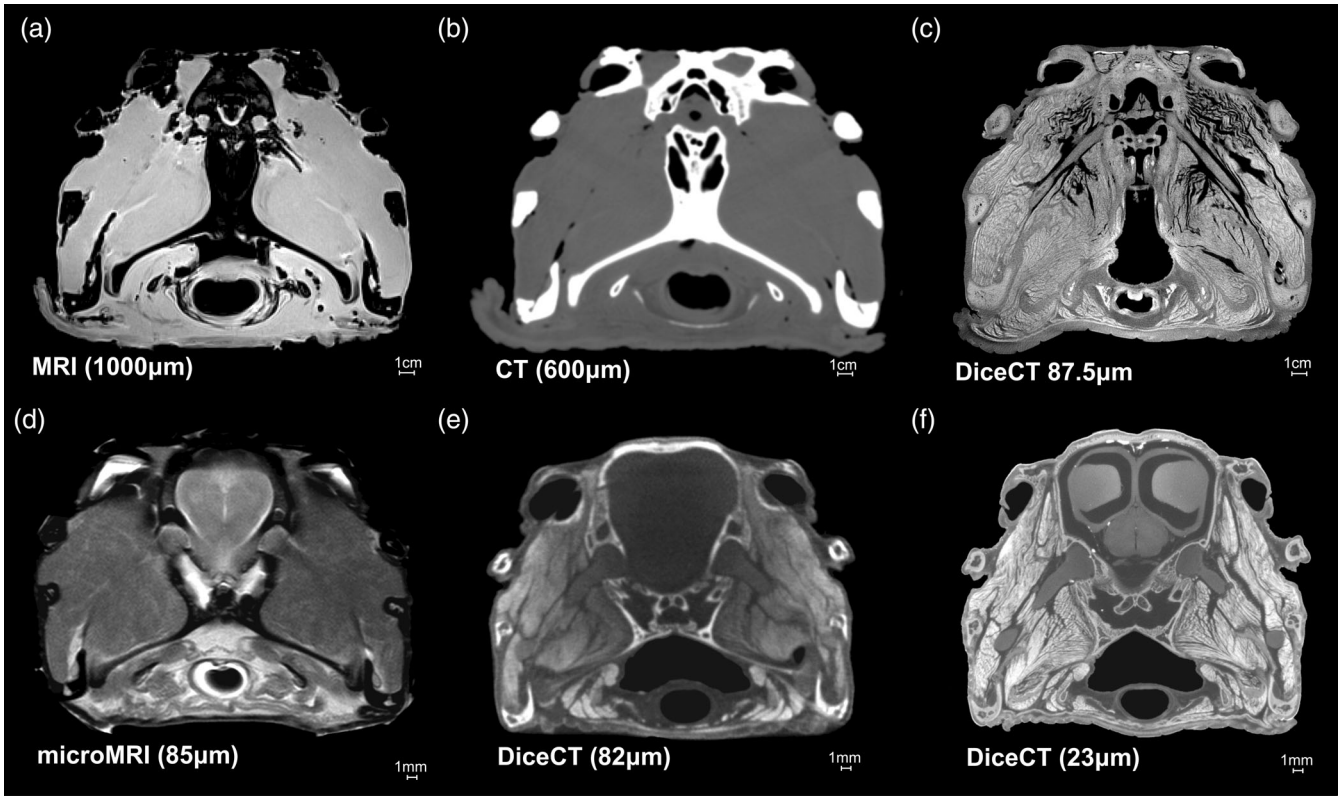

FIGURE 1 Imaging modalities and contrast offer a variety of views into the heads of *Alligator mississippiensis*, here using axial slices through the trigeminal fossa and ganglion. (a) Medical MRI of adult MUVC AL22. (b) Medical CT of adult MUVC AL22. (c) Iodine contrast enhanced microCT of adult MUVC AL606 (87.5 µm). (d) MicroMRI of hatchling MUVC AL31 (85 µm). (e) Iodine contrast enhanced microCT (83 µm) of hatchling MUVC AL31. (f) Iodine contrast enhanced microCT (23 µm) of hatchling MUVC AL31

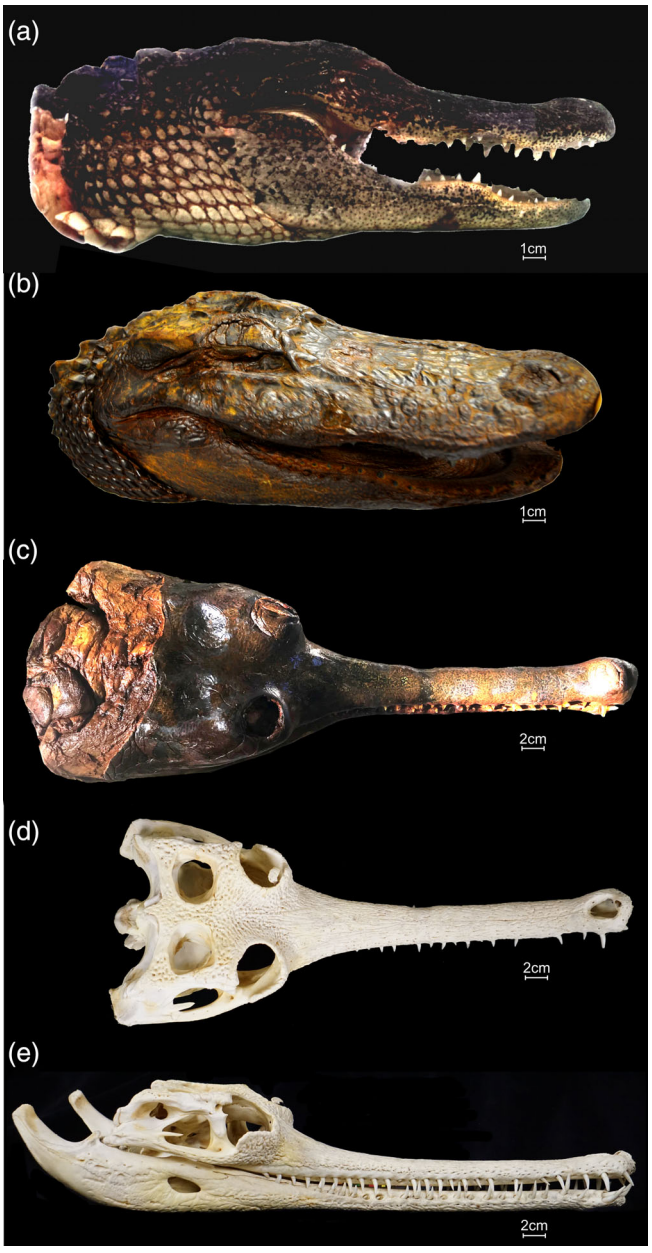

FIGURE 2 Large specimens of crocodilians during preparation before, during and after iodine contrast. (a) *Alligator* MUVC AL606 during formalin fixation, right lateral view. (b) *Alligator* MUVC AL606 after immersion in I_2KI, right oblique lateral view. (c) Gharial TNHC 110000 after I_2KI injections, dorsal view. (d) *Gavialis gangeticus* TNHC 110000 after skeletonization, dorsal view. (e) *Gavialis* TNHC 110000 after skeletonization, right lateral view

and preserved museum specimens (Figure 5). Using 3D modeling and computational approaches, we estimate volumes, calculate 3D jaw muscle vectors, and visualize muscle fibers, that then act upon the skull during feeding behaviors (Figures 6–8). These models can be shared widely through online digital repositories (Figure 9).

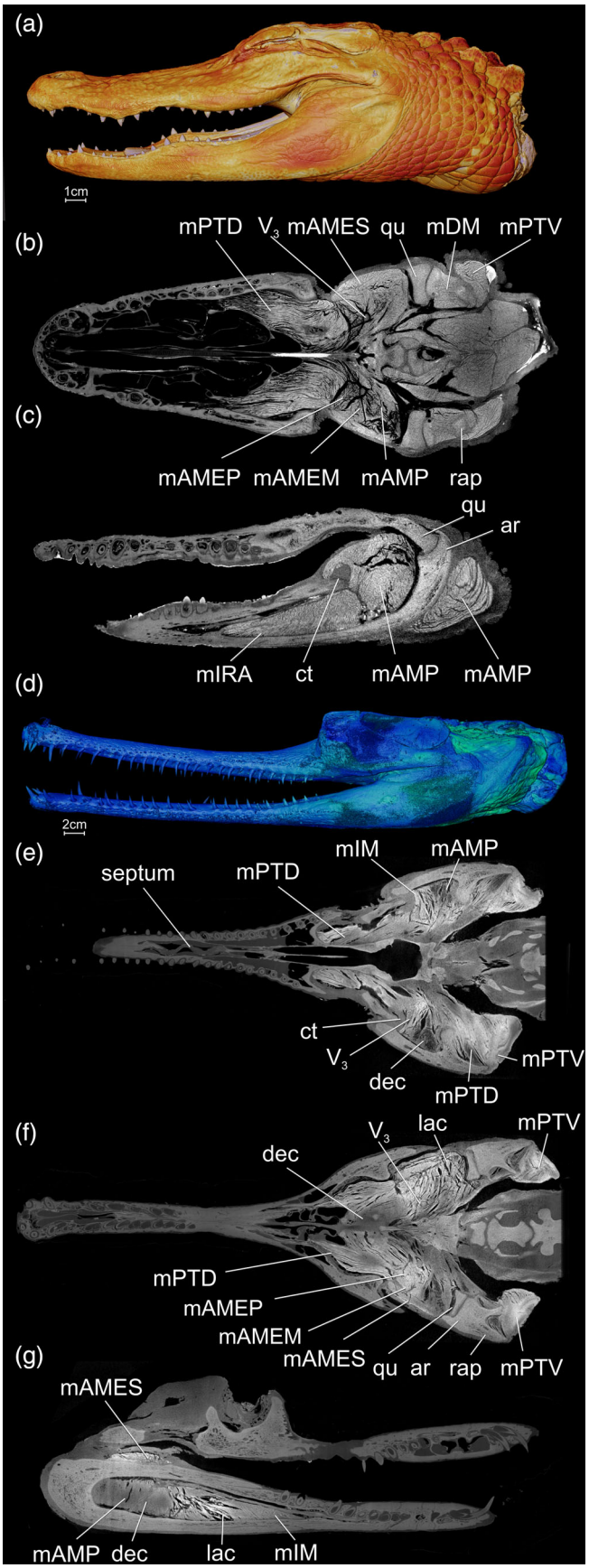

FIGURE 3 Legend on next page.

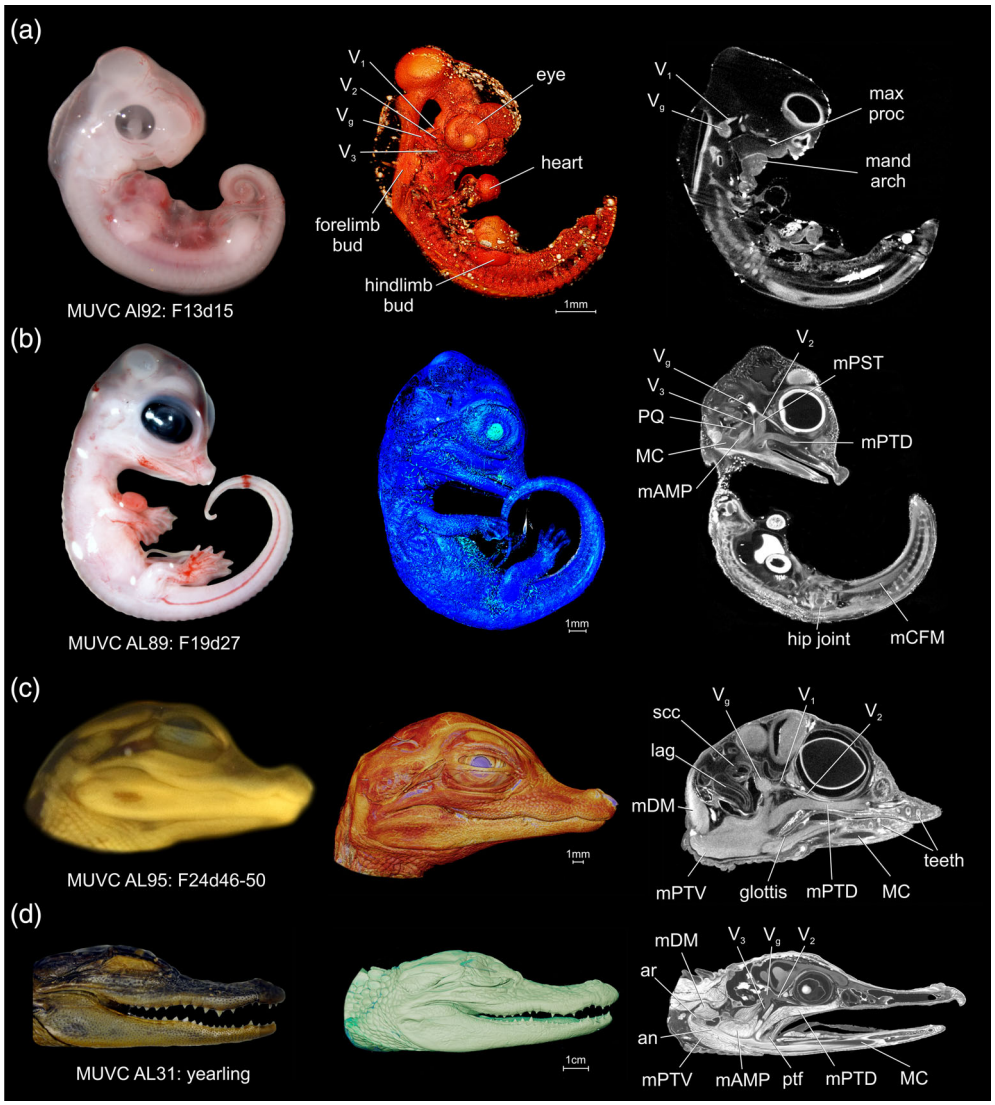

FIGURE 4 Contrast imaging offers new opportunities to study the development and ontogeny of soft tissue systems. For example, these data of a partial ontogenetic series of *Alligator mississippiensis* in right lateral views, illustrate key organs, trigeminal nerves, and jaw musculature. Left: Photograph. Middle, volume rendering. Right, parasagittal section. (a) MUVC AL92, Ferguson stage 13, day 15. (b) MUVC AL89, Ferguson stage 19, day 27. (c) MUVC AL95, Ferguson stage 24, day 46–50; MUVC AL31, yearling

Together, these approaches help clarify patterns in jaw muscle topology and ontogeny, fiber architecture and function, and diversity of muscle anatomy across this wonderful clade of vertebrates.

FIGURE 3 Iodine contrast offers extraordinary views into the heads of crocodylians including anatomical features of cartilages, nerves, and muscles of large specimens such as a large alligator (MUVC AL606) and gharial (TNHC 110000) specimens. (a) Volume rendering of *Alligator* MUVC AL606 in left, lateral view. (b) Horizontal section of *Alligator* MUVC AL606 through nasal cavities and occipital condyle. (c) Parasagittal section of *Alligator* MUVC AL606 through m. intramandibularis and adductor chamber in left lateral view. (d) Volume rendering of *Gavialis* (TNHC 110000) in left, lateral view. (e) Horizontal section of *Gavialis* (TNHC 110000) through ventral nasal cavity and ventral adductor chamber. (f) Horizontal section of *Gavialis* (TNHC 110000) through dorsal nasal cavity and middle adductor chamber. (g) Parasagittal section of *Gavialis* (TNHC 110000) through right adductor chamber in right lateral view

2 | CONTRAST IMAGING

Iodine and other contrast agents for soft tissues such as muscles, nerves, and vasculature are popular tools for visualizing soft tissues of arthropods, vertebrates, and other animals using X-ray computed tomography (CT; Metscher 2009; Gignac et al., 2016; Holliday et al., 2019; Lessner and Holliday, 2020). Like many others, we have had great success in contrast imaging a variety of specimens including the heads and limbs of animals that fit inside microCT instruments. Although medical CT also works with iodine-contrast data (Figure 1c), the resolution of these scans (~600 μm^3) does not lend much added value to the data aside from gross arrangements of structures and is only effective with larger specimens. Crocodylian heads are relatively robust against the effects of contrast staining as their skulls are more resilient to the effects of dehydration, shrinkage, and plastic deformation, which are common side effects of I_2KI staining (Vickerton et al., 2013; Li et al 2015; Hedrick et al., 2018;

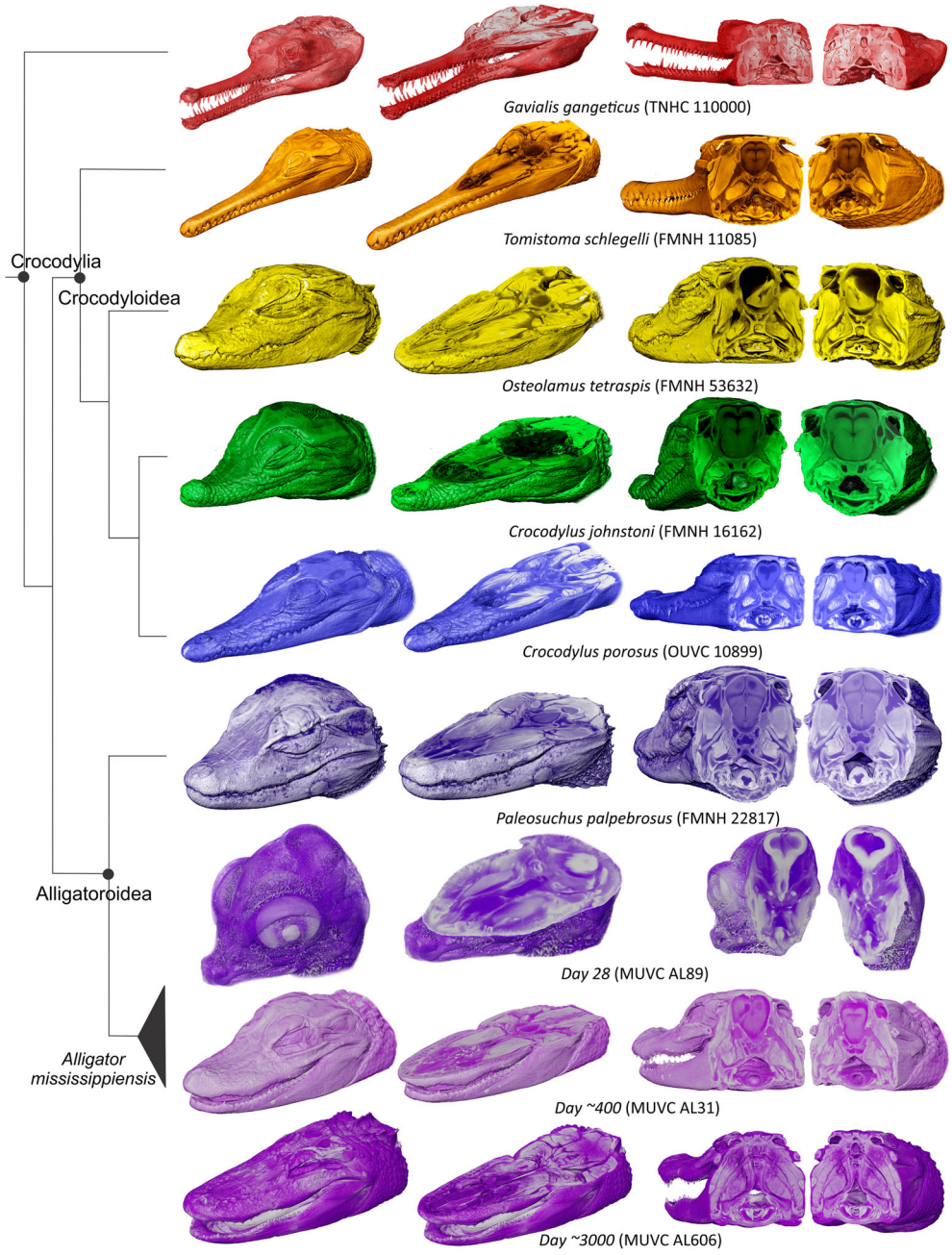

FIGURE 5 This cladogram illustrates a diversity of contrast-enhanced and imaged crocodylian species. Increased sampling of soft tissues will improve detecting biomechanical, ontogenetic, and phylogenetic patterns in crocodylian cranial evolution

Early et al. 2020). Because bones of the skull tend to remain rigid, the jaw musculature spanning the elements and their interweaving neurovasculature also largely retain their correct and largely undistorted anatomies (Figure 1). These qualities lie in contrast to the more fragile or deformable skulls of birds, lizards, snakes, and embryos, which often require closer attention or additional steps in stabilization (Wong et al., 2013; Gignac and Kley, 2014; Gignac et al., 2016; Early et al., 2020; Lessner and Holliday, 2020). Therefore, we have experienced considerable success in our treatments of crocodylian heads.

The most common and passive way to introduce contrast into specimens is to immerse them in solutions for periods of time with agitation (Metscher 2009; Gignac et al., 2016; Lessner and Holliday 2020). However, diffusion gradients become barriers to getting good contrast in deep tissues such as the cores of jaw muscles or brains (Li et al. 2015). To remedy these challenges, Iodine contrast solutions can be introduced into specimens through direct injections as well as vascular catheterization with near-immediate effects. These infusions work on both fresh and formalin-fixed specimens. For example, Tsai and Holliday (2016) hand-injected iodine with a needle

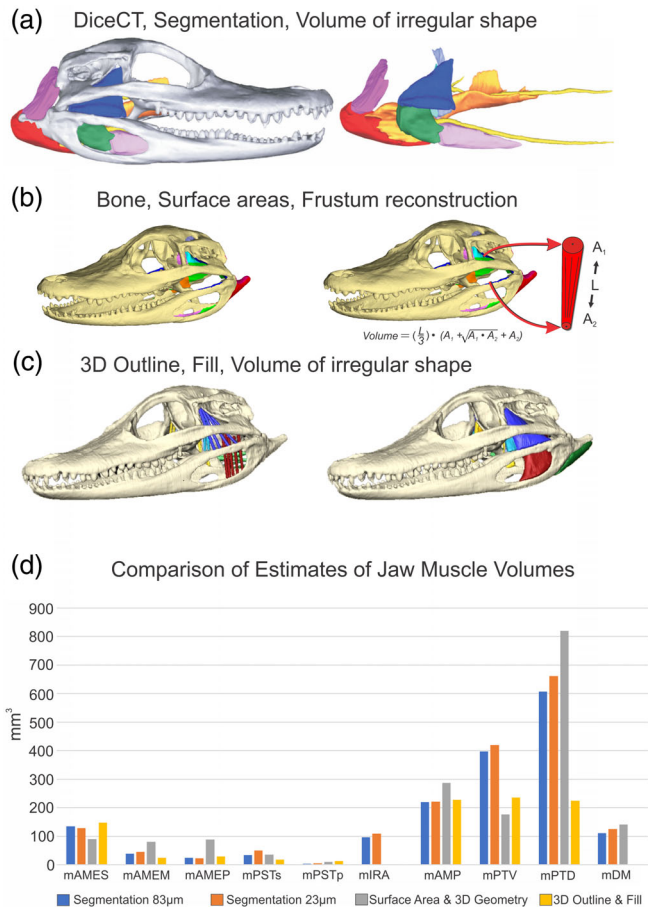

FIGURE 6 Variation in muscle modeling approaches. The same specimen of *Alligator* (MUVC AL31) was used by multiple investigators to estimate the volumes of jaw muscles using different modeling methods. (a) MUVC AL31 was DiceCTed, imaged at 83 µm and segmented in 2012 (Holliday et al., 2013); the same specimen was re-immersed in iodine, and rescanned at 23 µm and re-segmented in 2019. (b) MUVC AL31 had its muscle attachments painted on a model of the skull. Muscle attachments were used to estimate the volume using a simple equation of a frustum (Sellers et al., 2017). (c) A series of cylinders were positioned in a model of the skull to outline perimeters of muscle bellies and then filled to calculate volume. (d) Comparisons of volumes using these different modeling methods. Frusta of large, complex muscles like mPTD likely require refinement to more accurately approximate muscle volumes

and syringe into the preserved hip of a large alligator while it was positioned on the gantry of a medical CT scanner. Scans had shown deeper tissues were still not satisfactorily perfused, but injection of fresh solution successfully revealed deeper tissues in the joint capsule within minutes. Ethanol-preserved specimens have proven resilient to repeated staining and scanning, giving promise to the imaging of museum specimens and other specimens in long-term storage. Stained specimens can be immersed in fresh ethanol solutions or sodium thiosulfate solutions (Gignac et al., 2016; Early et al., 2020) to leach iodine out of the specimens with considerable thoroughness, making the staining, imaging, and destaining of museum specimens less destructive than conventional dissection methods. Staining and destaining both carry risks of demineralization and chemical alteration of bone (Early et al., 2020; Dawood et al., 2021), which can be mitigated with care. For example, a hatchling alligator head (MUVC AL31) featured in Holliday et al., (2013), Sellers et al., (2017) and Lessner and Holliday (2020) has proven resilient to re-immersing and re-imaging over the course of years as microCT resolution and specimen fit has increased from ~82 to ~23 µm (Figures 1e, f, 4). New details of the same specimen are now revealed by the increased resolution and so finer branches of the same nerves can be segmented (Lessner and Holliday 2020), the muscles are now more amenable to 3D fascicle tracking (e.g., Jeffery et al., 2011; Kupczik et al., 2015; Dickinson et al., 2018; Sullivan et al., 2019; Katzke et al., 2022; Figures 7, 8), and the overall accuracy of segmented structures is increased.

Contrast imaging of large specimens (e.g., diameter ~8 cm and greater) can be challenging. Long diffusion distances to deep tissues can take months when using passive approaches like long-term immersion (Li et al., 2015). Large specimens and their containers are too heavy for most bench-top shakers thus consistent agitation is harder to achieve than with smaller specimens and vessels. Incomplete penetration of formalin or iodine can result in pockets of decomposed, unpreserved tissues, or unstained tissues. Thus, catheterization of vessels or direct injections of solutions into deeper tissues can complement and accelerate perfusion of fixative or contrast. Larger specimens are also more challenging to fit in many high-resolution scanners and only a few instruments are available for this scale of specimen (e.g., University of Texas UTCT Facility).

We have had considerable success with contrast staining and imaging larger, historical museum specimens, recently fixed specimens, as well as large, unfixed specimens of crocodylians at the University of Texas at Austin UTCT facility. To capture the internal anatomy of the head of an adult alligator (MUVC AL606) (Figure 1c), we immersed an ~18 cm-long head in a covered, 30-gal aquarium of 10% NBF for approximately 8 months (Figure 2a,b). The specimen was medical CT-scanned and then moved to a five-gallon bucket of 5% I2KI Ethanol solution for an additional 8 months. Solution was changed out as the opacity declined and the bucket was agitated occasionally. A test medical scan revealed several pockets of tissue that remained unstained, and so I_2KI solution was directly injected into some deeper portions of the temporal region of the specimen (Figures 1c, 3).

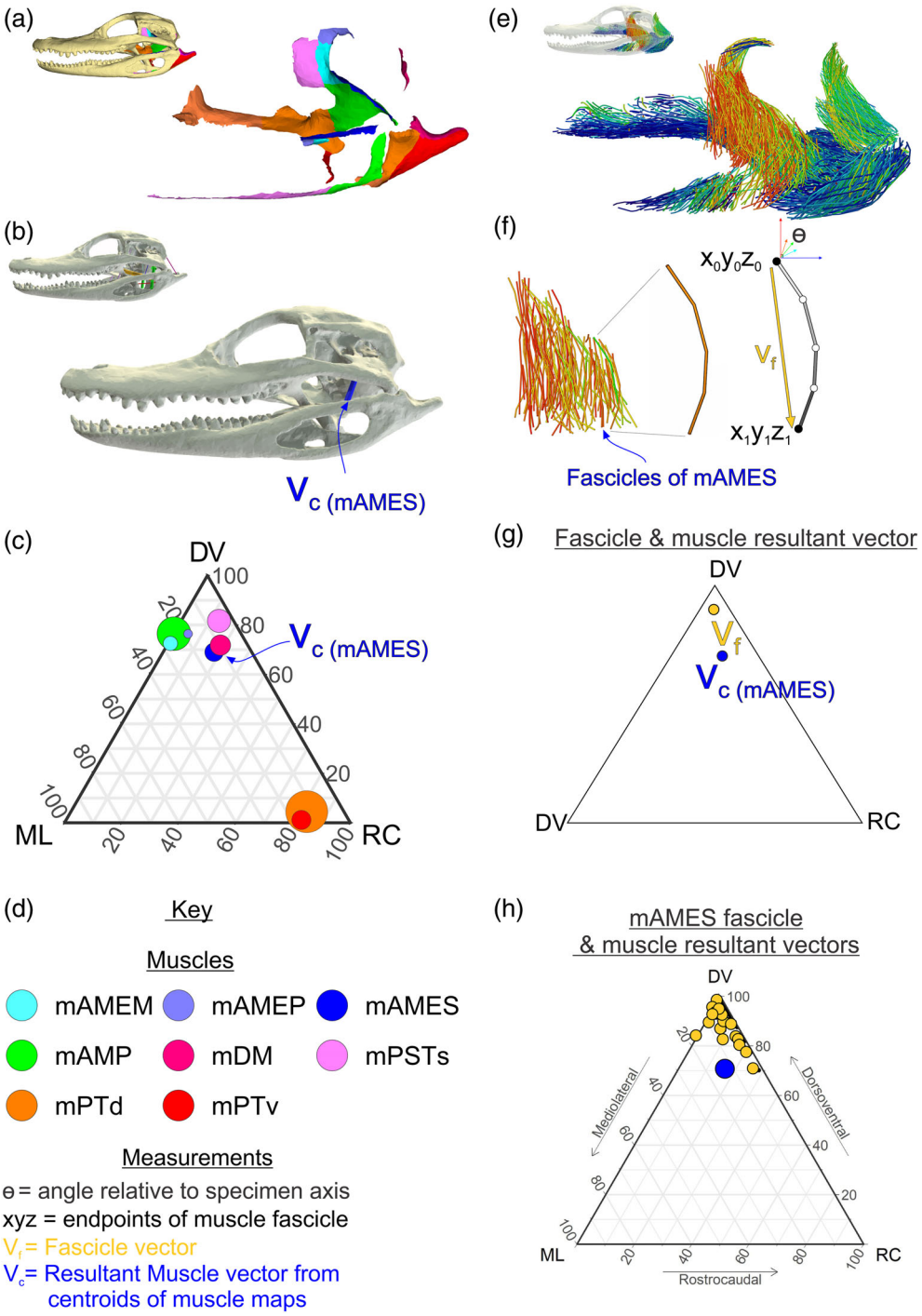

FIGURE 7 Introduction to modeling muscle resultants and fascicle vectors in 3D. (a) *Alligator*, (MUVC AL31) 3D muscle maps in left, lateral view. (b) 3D modeled resultant vectors of jaw muscles highlighting the resultant of mAMES. (c) 3D resultant vectors of jaw muscles projected into ternary space illustrating the different orientations and scaled forces. (d) Key for jaw muscle colors and abbreviations used in vector calculations; (e) model of 3D muscle fascicles of MUVC AL31 in left lateral view. (f) Illustration of measurements used to calculate muscle fascicle vectors of individual muscle fascicles. (g) Vectors of a select muscle fascicle (fascicle vector) from mAMES plotted with the 3D resultant muscle vector of mAMES. (h) all 3D fascicle vectors and resultant muscle vector of mAMES illustrate the clustering and directionality of fascicles are similar in orientation of the muscle resultant, exemplifying a largely parallel fibered, dorsoventrally oriented muscle

The specimen was then scanned again at 87.5 μm at UTCT to discover that the tissues had been successfully stained. These new data are the first to reveal the internal anatomy of an adult alligator and can be used to compare changes in jaw muscle sizes and orientations during ontogeny, compare relative sizes of nerves over age, as well as identify differences in attachments and architecture across different species of crocodylians (Figures 3a–c, 5). The specimen remains preserved in 70% ethanol.

Particularly, large specimens that cannot be formalin-fixed for long-term study offer numerous challenges. In Winter 2018, a 63-year-old adult female gharial ("Louise") passed away at the Ft. Worth Zoo (Weigl, 2014). The University of Texas at Austin Biodiversity Collections wished to preserve the specimen (TNHC 110000) as a skeleton but agreed to allow us to try to contrast stain and scan the head and neck prior to skeletonization. Skeletonization of formalin-fixed specimens is inherently difficult, so we

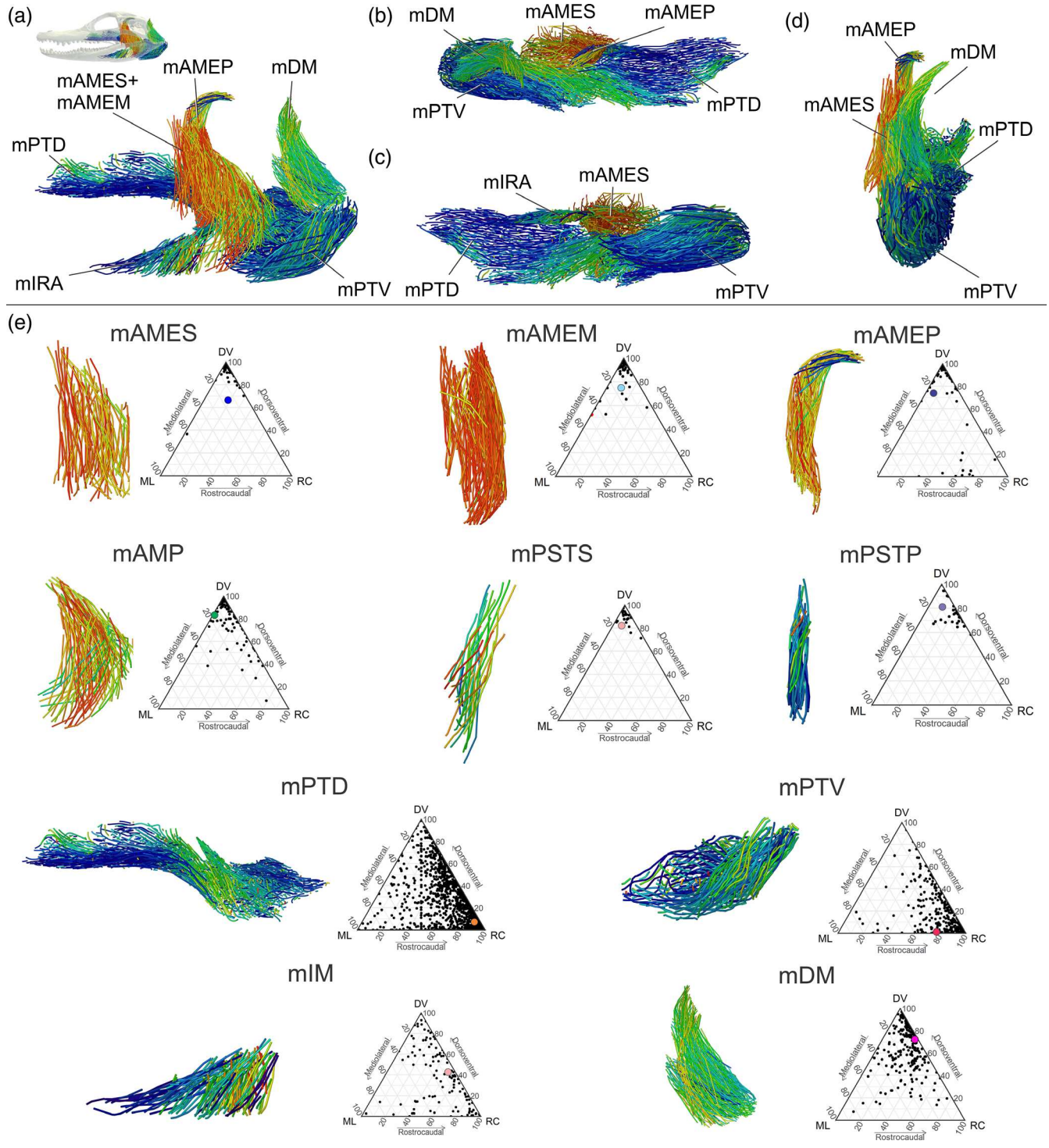

FIGURE 8 Atlas of 3D muscle fascicle architecture of *Alligator mississippiensis* MUVC AL31. Segmented muscles from DiceCT data of alligator (MUVC AL31) were autosegmented and their vectors plotted in ternary space to show clustering patterns of fascicle vectors and muscle vector resultants derived from muscle map centroids to illustrate patterns of pennation in jaw muscles. See Figure 7 for explanation. (a) Left, lateral view; (b). Dorsal view. (c) Ventral view. (d) Caudal view. (e) 3D fascicle models of individual jaw muscles in left, lateral view with ternary plots with fascicle vectors and muscle resultant vectors

were faced with trying to inject iodine solution into the freshly thawed head of the gharial. Catheterization of the carotid artery and jugular veins in the neck worked for a brief time but eventually failed as vascular tissues deteriorated from physical handling. From there, we decided to hand inject boluses of Iodine solution directly into the soft

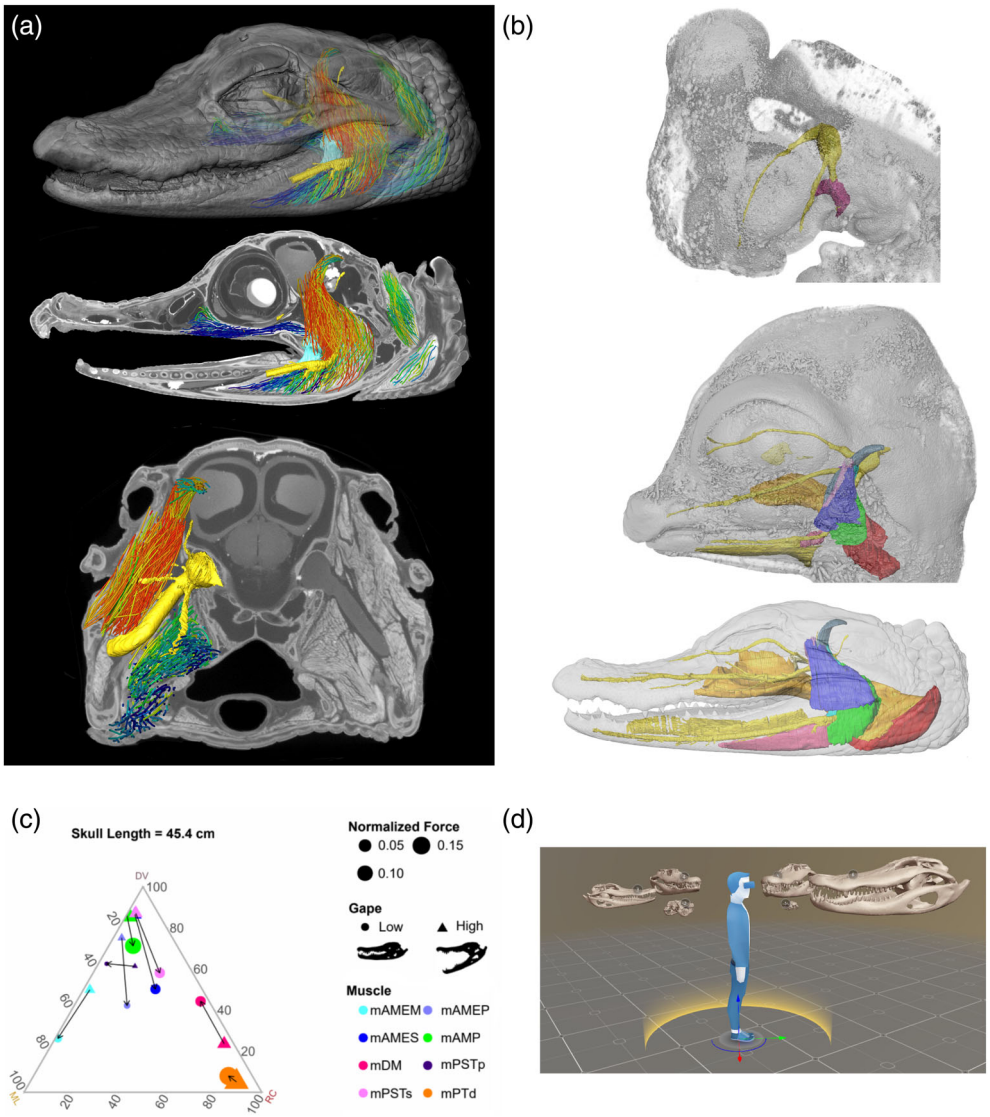

FIGURE 9 Future directions in imaging and biomechanics of crocodylian jaw muscles. (a) Combining multiple modalities of imaging and modeling approaches can reveal anatomy unlike that seen before. (b) Segmentation of jaw muscles and other soft tissues can reveal patterns in development and ontogeny. (c) Comparing changes in muscle resultants during jaw closing reveals patterns in jaw muscle and skull mechanics. (d) Migrating models to augmented and virtual reality platforms can enrich the education of people around the world such as our face-to-face with alligators environment (e.g., https://sketchfab.com/holliday)

tissues using 10-cm long spinal tap needles fixed to 50 cc syringes. Over the course of two 4-day sessions, we hand-injected iodine solution directly into the gharial (Figure 2C). This process resulted in approximately 500 individual injections of about 20 L of ~7% I_2KI and H_2O solution. We used test scans at the UTCT facility to identify regions that needed to be further targeted as well as to monitor a growing pocket of decomposition in the tissues between the orbits and the palate. Although many regions of the musculature and head were easy to target with this approach, others were still out of reach. For example, to inject solution into crevices like the Meckelian fossa of the dentary, filled with m. intramandibularis, we slid a needle obliquely through the external mandibular fenestra, along the inner surface of fossa, bending the needle along the way. Other pockets of tissue were equally challenging to gain approach using a needle including the nasal cavity, rostral region of the ventral jaw joint where mAMP inserts, and encephalic cavity (Figure 3). Eventually, the balance between introduced contrast and emerging decomposition warranted final scanning. Again, the UTCT facility is the only one in North America with a gantry large enough to fit a specimen the size of a gharial head, and the ability to scan the specimen at a resolution that can reveal muscle architecture and other finer anatomical details.

Ultimately, TNHC 11000 was scanned whole at 117 μm, as well as a mosaic (snout, left skull, right skull) at 75 μm and stitched together revealing incredible new views of internal anatomy of this rarely studied crocodilian species (Figures 3, 5). A growing pocket of decomposition is visible in the midline palatal region and in a pocket rostroventral to the jaw joint. Also visible are numerous punctures in the soft tissues made by the needles used to inject contrast, but these only minimally detract from the overall value of the data. After scanning was completed, the specimen was then flensed of soft tissue and soaked in water for 1 week with daily water

changes to remove excess iodine. The roughly cleaned head was dried and placed into a dermestid beetle colony for approximately 2 months. Once the soft tissues were removed, the bones were soaked in a bath of ~5% aqueous ammonia for 1 week, followed by a week-long bath in water that was changed daily. The prepared skull is a natural bone color with only a few localized regions that were stained brown from iodine (Figure 2d,e). These stains have continued to subside. We found no damage to the bones caused by the needles such as in the Meckelian fossa or other portions of the braincase we know we sometimes scraped against during injections, although some scoring was introduced during flensing. These results are incredibly promising for similar treatments of other fresh specimens intended for skeletonization in museum collections.

Alligator and crocodilian embryos have proven resilient to contrast staining as well. Like all embryos, these specimens are at greater risk of dehydration and plastic deformation than more rigid specimens of adult species (Figure 4a,b). Lessner and Holliday (2020) had success reducing deformation in alligator embryos using a modified STABILITY protocol (Wong et al., 2013; Carlisle et al., 2017) followed by immersion in I_2KI solutions and mounting in agarose gel to minimize movement during CT scanning. Other solutions produce similar contrast in embryos (e.g., phosphotungstic acid [PTA] and phosphomolybdic acid [PMA]) require longer staining durations than iodine because of larger molecule sizes (Descamps et al. 2014, Metscher 2009). Factors influencing scan quality in embryonic alligators (i.e., head length of 3.8–31 mm) include: stain concentration (1% w/v I_2KI is sufficient to stain while minimizing deformation); stain duration (20 h allows for stain penetration while minimizing overstaining); and scan resolution (13–28 μm voxel size was adequate for viewing structures as small as 50 μm). Contrast imaging of embryonic material (Figure 4) is capable of not only revealing musculature and neurovascular tissues but also cartilaginous structures of the chondrocranium, ossifying bone, and connective tissues.

3 | SEGMENTATION AND VOLUMETRIC ESTIMATES

Contrast imaging data can provide the foundation for higher order analyses of musculoskeletal biomechanics, physiology, and evolution. Dissection-based studies of musculature rely on manipulation and visual observations of morphology. But despite their primacy, these methods can be destructive or otherwise modify the muscles under study including separation of connective tissues and muscle fibers from their attachments, displacement of neurovasculature and other elements and ultimately removal or destruction of tissues, precluding the study of, for example, museum specimens of rare or endangered species. Contrast imaging offers insights into many of these same gross features in situ and like dissection-based approaches, enables the digital isolation of soft-tissue structures and measurements of them including surface areas of attachments (Grosse et al., 2007; Davis et al., 2010; Sellers et al., 2017; Cost et al., 2020), volumes (Holliday et al., 2013; Lautenschlager 2014), muscle arrangement (Lautenschlager et al., 2017), and potentially properties of muscle architecture (Dickinson et al. 2018; Sullivan et al., 2019; Katzke et al., 2022; Figures 7, 8).

Like dissection-based observations of muscle anatomy, observations of contrast data and their interpretations may differ among investigators. Furthermore, different 3D modeling methods can result in different estimates of volumes or other parameters. Finally, even imaging the same specimen at later dates, such as when scanning resolutions improve, result in different interpretations of morphology. To briefly illustrate variation in muscle estimates, we show how 3D modeling methods differ in their estimates of muscle anatomy among individuals, among different scans of the same individual and using different 3D reconstruction methods by different investigators (Figure 6).

First, the authors in Holliday et al. (2013) 3D atlas of *Alligator* muscles all took turns segmenting the same data (MUVC AL31; a hatchling alligator) that had been DiceCTed at ~82 μm. Each author varied in expertise and experience with alligator jaw muscles including an assistant professor with several relevant publications (Holliday), a doctoral student with comparative anatomy expertise (Tsai), a senior undergrad (Skiljan) with digital osteology experience and a High School student (Pathan) with minimal experience. The data proved remarkably challenging for the junior students to interpret but even the senior authors relied on one another's feedback to make best estimates of fascial planes and separations between named muscle bellies. This shows DiceCT data, particularly that of crocodilian jaw muscles, can be challenging to interpret even for seasoned anatomists.

Second, the same specimen used above (MUVC AL31) was subsequently reimmersed in I_2KI and scanned in 2018 at a higher resolution of 23 μm. This time, muscles were segmented Holliday and two new investigators, Sellers and Verhulst, both of whom had significant experience in crocodilian anatomy and experience in DiceCT of jaw muscles of birds respectively, along with Holliday. This group found slight but unsubstantial differences in the volumes of segmented jaw muscles. The pterygoideus muscles were found to be larger in the latter study

whereas the temporal muscles were found to be slightly smaller. There were no clear differences in particular interpretations of the muscle bellies. The higher resolution data made the boundaries of muscles, bone, nerves, and other soft tissues more refined and visible suggesting this latter segmentation may be more accurate than the former.

Third, to illustrate how different modeling approaches estimate muscle volumes from bony data, akin to a study of fossils, for example, the 3D model of the skull of MUVC AL31 (83 μm) was shared with co-author Lautenschlager, who has similar expertise in crocodilian cranial anatomy as Sellers and Holliday (Figure 6). Here, we used simple and complex polyhedrons to estimate volumes of the jaw muscles in two different ways. Sellers used Strand7 (G1D Computing Pty Ltd, Sydney, Australia) to map surface areas of muscles reflecting their bony attachments (sensu Grosse et al., 2007; Davis et al., 2010; Sellers et al., 2017, Cost et al., 2020; Cost et al., 2022; Sellers et al., 2022) and then the centroids and surface areas of the origins and insertions were used to calculate the volume of a frustum (Sellers et al., 2017), a relatively simply shape. Meanwhile, Lautenschlager employed their outline & fill (O&F) method, where, using Avizo (Thermo Fisher Scientific), the estimated boundaries of muscle attachments were marked and connected by a series of narrow cylinders (Lautenschlager 2013). These simplified point-to-point connections were subsequently inspected for intersections between the cylinders and between cylinders and bone. If intersections occurred, the attachment sites were adjusted slightly to allow all cylinders to fit within the adductor chamber. In a final step, the cross-sections of the cylinders were increased manually to merge cylinders representing the same muscle using the region growing tool in Avizo's segmentation editor. The cross-sections were grown continuously until they encountered other muscles or bone.

Although the segmented DiceCT muscle data offered precise estimates of muscle volumes, the 3D modeling using polyhedrons varied in their performance. The Outline and Fill method found relatively similar volumes as the segmented DiceCT volumes for muscles that were considerably constrained by the skull architecture, such as the temporal muscles. But the O&F method found rather different volumes of the pterygoideus muscles, underestimating the volume of mPTV by nearly half and even more so the volume of mPTD. These muscles are poorly constrained by the surrounding bone and were therefore more prone to subjectivity and interpretation during the modeling process. The frustrum method found similar volumes for the temporal muscles as the DiceCT and O and F approaches although mAMEM (adductor mandibulae externus medialis) was found to be relatively larger. The frustum method substantially overestimated the volume of mPTD compared with volumes determined from DiceCT and O and F methods but underestimated the volume of mPTV. The disparity in volume estimates of mPTD using both O and L and Frustum modeling methods are likely due to the muscle's complex attachments along the face, interorbital septum, and braincase. This broad attachment, the muscle's wrapping along the inner surface of the palate and indirect course toward its mandibular attachment is ignored by the single frustum method, which instead, simply clips through the shape of the cranium toward the mandible. The under-reporting of the mPTV is because the extensive tendinous attachment of mPTV that is not represented by bony surface as well as via similar clipping artifacts as present in the reconstruction of mPTD.

4 | 3D JAW MUSCLE RESULTANTS AND MUSCLE ARCHITECTURE

Segmentation, visualization, and estimates of muscle volumes offer incredible new insights into anatomy and function. These data enable further exploration into muscle mechanics by combining estimates of muscle attachments, muscle volumes and even muscle architecture (Figures 7, 8). We have previously shown that 3D muscle resultants can be accurately derived from 3D muscle attachment mapping and frustum-based volume estimates to estimate bite forces in *Alligator mississippiensis* (Sellers et al., 2017) and that these muscle resultants can be used to track changes in cranial performance among sauropsids (e.g., Cost et al., 2019; Wilken et al., 2019; Wilken et al., 2020; Cost et al., 2022) and during suchian evolution (Sellers et al., 2022).

Complementing these estimates, we can now also use segmented volumes of DiceCT jaw muscles to model the architecture of muscle fibers within each muscle akin to those modeled in the flight muscles of European starlings (Sullivan et al., 2019). Briefly, using machine learning approaches in Avizo Xfiber (Thermo Fisher Scientific), we can train the software to recognize individual muscle fibers within the data and automatically segment them and colorize their angular relationships relative to the organism or other axes (Figures 7, 8). These objects also carry 3D coordinate data that can be compared and reported in a variety of ways. Automated methods like this offer particular benefits over hand-segmented muscle fascicles. Most importantly, it saves time and is generally holistic, capturing all available fascicles in one sample in just a few hours of computational work whereas hand-segmenting thousands of individual fascicles, in our alligator, for example, might take hundreds of person-hours of effort. That said, determining how well-automated

methods capture true morphology is still under study by a variety of researchers (Dickinson et al. 2018; Khalife et al., 2018; Sullivan et al., 2019; Dickinson et al., 2019; Katzke et al., 2022) and even the data presented here (Figure 8) are worthy of further refinement. Noise is introduced by specimen preservation, preparation, imaging parameters, machine learning parameters, connective tissue, interweaving neurovasculature, and other sources. Thus, hand-segmented data, where the trained eye can discriminate noise from fascicles, may be superior in some circumstances where person-hours are less limiting.

We can quantify vectors of 3D muscle fascicles using the two endpoints of each fascicle, thereby mimicking the orientation of a straightened muscle fascicle (V_f; Figure 7d). These values make for estimated projection of muscle fascicle orientation but may ignore fusiform, bulging shapes of muscles, or important, curved paths the fascicles might take if they happen to wrap around structures like the pterygoid bone or retroarticular process, or even other soft tissues such as eyeballs and other muscles. Regardless, fascicle vectors illustrate patterns of pennation, where like a unimodal versus bimodal curve, parallel-fibered muscles tend to have fascicle vectors that cluster in on a particular region of a ternary plot, whereas pennate muscles will have fascicles that cluster in more than one region of a ternary plot (Figure 8). For example, some temporal muscles of *Alligator* have largely parallel-fibered muscles and thus the fascicles of mAMES largely occupy narrow regions of fascicle vectors (Figure 7). Alternatively, m. pterygoideus dorsalis (mPTD) has several bellies arising from inside of the face and palatal region, resulting in a broad, diversity of fascicle vectors reflecting the muscle's complex architecture (Figure 8).

We can further demonstrate the functional anatomy of a muscle by combining our 3D muscle resultant vectors determined from muscle maps (Figure 6), projected upon muscle fascicle vectors (Figures 7, 8). For example, m. depressor mandibulae (mDM) is largely a parallel-fibered muscle, where the orientations of muscle fascicle vectors are similar to the 3D muscle resultant (Figure 8). On the other hand, whereas the muscle fascicles of mAMEM are largely oriented in a similar direction, the overall 3D resultant of the muscle, the colored circle, is adjacent to the nesting of muscle fascicle vectors (Figure 8). This demonstrates that this muscle is unipennate, where clusters of muscle fascicles are similarly oriented, but not necessarily parallel with the 3D resultant of the muscle overall. This fascicle pattern reflects the anatomy of the mAMEM, where numerous fascicles arise from the cranial adductor tendon on the muscle's caudomedial border (Schumacher, 1973; Holliday and Witmer 2007). Finally, the broad distribution of muscle fascicle vectors in mPTD, compared with the largely horizontal 3D muscle resultant, demonstrate the complex architecture of this muscle, which is responsible for generating most of the bite force in alligators and crocodilians (Gignac and Erickson 2016; Sellers et al., 2022). Altogether, these new methods of visualizing and modeling muscle shape, size and pennation not only enable promising, fascinating, and stunning new visions of myology, but also, once integrated with behavioral and shape analyses, inform patterns of mechanical advantage, cranial performance, and evolution of the feeding apparatus in crocodilians. Challenges remain regardless. When met with even a "simple" muscle like a starling supracoracoideus muscle, we were taken aback by how much complexity in architecture was beneath the surface of classically "bipennate" muscle (Sullivan et al., 2019). Here we show we can relatively easily segment and visualize muscle architecture of notoriously complex alligator jaw muscles. However, summarizing the functional morphology of the architecture, such as through ternary plots here, still requires new tools and it remains difficult to compare 3D muscle architecture parameters across individuals or species without abstracting away all of the complexity. Indeed, learning more about the internal architecture of a muscle via in situ imaging, as opposed to "superficial-to-deep" dissection, reveals how little we actually understand about its morphology and function.

5 | NEW DIRECTIONS

We are on the precipice of an inspiring renaissance in musculoskeletal imaging and computational biology that will undoubtedly reveal new discoveries in not only crocodilian evolutionary biology but also that of other animals. Here, we have illustrated how contrast imaging approaches can be used to capture unique anatomies of exotic and model animal species such as gharials and alligators. Although challenges arise when imaging fragile embryos or unfixed specimens, data derived from them prove invaluable for understanding the development and diversity of living species. These data are critical to capturing vertebrate craniofacial diversity, and we can now model multiple organ systems together in ways that approach anatomical reality such as combining trigeminal nerve models (e.g., Lessner & Holliday, 2020) with 3D pennation models of jaw muscles (Figure 9a). We expect these imaging data will facilitate numerous new avenues of investigation, including tracking the development and ontogeny of alligator jaw muscles (Figure 9b), their functional relationships with the skull, and how to best estimate muscle physiology in extinct crocodyliform species during behaviors like jaw closing (Figure 9c).

Here, we provided several examples of how 3D modeling, muscle mechanics, and data visualization can elucidate patterns among different jaw muscles and their predicted performances. Although these methods are superior to muscle reconstructions using other approaches, such as the Outline and Fill method, to quantify muscle properties, they are generally not applicable to fossil specimens. However, the improved resolution and amount of data obtainable from the new imaging techniques can be used to inform muscle models in fossil animals (e.g., Lautenschlager et al., 2017). Because this technology is still emerging, we expect many improvements to workflows, automation, and data visualization that will capture the complicated morphology and functional environment of jaw muscles, the joints they cross and the skulls they load. Additionally, 3D model hosting sites like Sketchfab (https://sketchfab.com/holliday/collections) offer the general public access to interactive and annotated models of crocodylian anatomy with options for virtual reality (Figure 9d). Finally, these models are more readily accessible and widely shareable thanks to online digital repositories such as Open Science Framework, which hosts much of our crocodylian data as CrocNet (https://osf.io/jmpck/) and Morphosource.

AUTHOR CONTRIBUTIONS

Casey Holliday: Conceptualization (lead); data curation (lead); formal analysis (lead); funding acquisition (lead); investigation (lead); methodology (lead); project administration (lead). **Kaleb C. Sellers:** Conceptualization (equal); data curation (equal); formal analysis (equal); funding acquisition (supporting); investigation (equal); methodology (equal); software (equal); visualization (equal); writing – original draft (equal); writing – review and editing (equal). **Emily Jesica Lessner:** Conceptualization (equal); data curation (equal); investigation (equal); methodology (equal); visualization (equal); writing – original draft (equal); writing – review and editing (equal). **Kevin M. Middleton:** Formal analysis (equal); funding acquisition (equal); investigation (equal); methodology (equal); resources (equal); software (equal); validation (equal); visualization (equal); writing – original draft (equal); writing – review and editing (equal). **Corrine Cranor:** Methodology (supporting); visualization (equal); writing – original draft (equal); writing – review and editing (equal). **Conner D Verhulst:** Investigation (equal); methodology (equal); visualization (equal); writing – original draft (equal). **Stephan Lautenschlager:** Investigation (equal); methodology (equal); visualization (equal); writing – original draft (equal). **Kenneth Bader:** Data curation (equal); investigation (equal); methodology (equal); resources (equal); writing – original draft (equal). **Matthew A Brown:** Data curation (equal); investigation (equal); methodology (equal); resources (equal); visualization (equal); writing – original draft (equal). **Matthew Colbert:** Investigation (equal); methodology (equal); software (equal); visualization (equal).

ACKNOWLEDGMENTS

We thank Ruth Elsey (Rockefeller State Refuge), Travis LaDuc (University of Texas), Diane Barber (Ft Worth Zoo), Alan Resetar (Field Museum), and Lawrence Witmer (Ohio University), for providing access to specimens. Funding was provided by NSF EAR/SEB 1631684, NSF IOS PMB 1457319; EAR-1762458, DBI-1902242, Missouri Research Board, University of Missouri Research Council; Jackson School of Geosciences Geology Foundation.

ORCID

Casey M. Holliday https://orcid.org/0000-0001-8210-8434
Kaleb C. Sellers https://orcid.org/0000-0002-3588-9562
Emily J. Lessner https://orcid.org/0000-0003-0774-1613
Kevin M. Middleton https://orcid.org/0000-0003-4704-1064
Stephan Lautenschlager https://orcid.org/0000-0003-3472-814X
Kenneth Bader https://orcid.org/0000-0003-2384-3150
Matthew A. Brown https://orcid.org/0000-0002-2713-1161
Matthew W. Colbert https://orcid.org/0000-0001-5710-7560

REFERENCES

Bailleul, A. M., & Holliday, C. M. (2017). Joint histology in *Alligator mississippiensis* challenges the identification of synovial joints in fossil archosaurs and inferences of cranial kinesis. *Proceedings of the Royal Society B*, *284*, 20170038.

Bona, P., & Desojo, J. B. (2011). Osteology and cranial musculature of *Caiman latirostris* (Crocodylia: Alligatoridae). *Journal of Morphology*, *272*(7), 780–795.

Bona, P., DeGrange, J. F., & Fernández, M. S. (2012). Skull anatomy of the bizarre Crocodylian *Mourasuchus nativus* (Alligatoridae, Caimaninae). *Anatomical Record*, *296*(2), 227–239.

Carlisle, A., Selwood, L., Hinds, L. A., Saunders, N., Habgood, M., Mardon, K., & Weisbecker, V. (2017). Testing hypotheses of developmental constraints on mammalian brain partition evolution, using marsupials. *Scientific Reports*, *7*, 4241.

Carr, A. N., Nestler, J. H., Vliet, K. A., Brochu, C. A., Murray, C. M., & Shirley, M. H. (2021). Use of continuous cranial shape variation in the identification of divergent crocodile species of the genus *Mecistops*. *Journal of Morphology*, *282*(8), 1219–1232.

Cost, I. N., Middleton, K. M., Sellers, K. C., Echols, S. M., Witmer, L. M., Davis, J. L., & Holliday, C. M. (2020). Palatal

biomechanics and its significance for cranial kinesis in *tyrannosaurus rex*. *The Anatomical Record*, *303*(4), 999–1017.

Cost, I. N., Sellers, K. C., Rozin, R. E., Spates, A. T., Middleton, K. M., & Holliday, C. M. (2022). 2D and 3D visualizations of archosaur jaw muscle mechanics, ontogeny, and phylogeny. *The Journal of Experimental Biology*, *225*, jeb243216. https://doi.org/10.1242/jeb.243216

Davis, J. L., Santana, S. E., Dumont, E. R., & Grosse, I. R. (2010). Predicting bite force in mammals: Two-dimensional versus three-dimensional methods. *The Journal of Experimental Biology*, *213*, 1844–1851.

Dawood, Y., Hagoort, J., Siadari, B. A., Ruijter, J. M., Gunst, Q. D., NHJ, L., Strijkers, G. J., de Bakker, B. S., & MJB, v. d. H. (2021). Reducing soft-tissue shrinkage artefacts caused by staining with Lugol's solution. *Scientific Reports*, *11*, 19781.

Descamps, E., Sochacka, A., De Kegel, B., Van Loo, D., Van Hoorebeke, L., & Adriaens, D. (2014). Soft tissue discrimination with contrast agents using micro-CT scanning. *Belgian Journal of Zoology*, *144*(1), 20–40.

Dickinson, E., Stark, H., & Kupczik, K. (2018). Non-destructive determination muscle architectural variables through the use of DiceCT. *The Anatomical Record*, *301*(2), 363–377.

Dickinson, E., Basham, C., Rana, A., & Hartstone-Rose, A. (2019). Visualization and quantification of digitally dissected muscle fascicles in masticatory muscles of Callithrix jacchus using non-destructive DiceCT. *The Anatomical Record*, *302*(11), 1891–1900.

Drumheller, S. K., & Wilberg, E. W. (2019). A synthetic approach for assessing the interplay of form and function in the crocodyliform snout. *Zoological Journal of the Linnean Society*, *188*(2), 507–521.

Early, C. M., Morhardt, A. C., Cleland, T. P., Milensky, C. M., Kavich, Q. M., & James, H. F. (2020). Chemical effects of diceCT staining protocols on fluid-preserved avian specimens. *PLoS One*, *15*(9), e0238783. https://doi.org/10.1371/journal.pone.0238783

Erickson, G. M., Lappin, A. K., & Vliet, K. A. (2003). The ontogeny of bite-force performance in American alligator (*Alligator mississippiensis*). *Journal of Zoology*, *260*, 317–327.

George, I. D., & Holliday, C. M. (2013). Scaling of the trigeminal nerve in *Alligator mississippiensis* and its significance for the evolution of crocodilian facial sensation. *The Anatomical Record*, *296*(4), 670–680.

Gignac, P. M., & Erickson, G. M. (2016). Ontogenetic changes in dental form and tooth pressures facilitate developmental niche shifts in American alligators. *Journal of Zoology*, *295*, 132–142.

Gignac, P. M., & Kley, N. J. (2014). Iodine-enhanced micro-CT imaging: Methodological refinements of the study of the soft-tissue anatomy of post-embryonic vertebrates. *The Journal of Experimental Zoology Part B*, *322*(3), 166–176.

Gignac, P. M., Kley, N. J., Clarke, J. A., Colbert, M. W., Morhardt, A. C., Cerio, D., Cost, I. N., Cox, P. G., Daza, J. D., Early, C. M., Echols, M. S., Henkelman, R. M., Nele Herdina, A., Holliday, C. M., Li, Z., Mahlow, K., Merchant, S., Muller, J., Orsbon, C. P., ... Witmer, L. M. (2016). Diffusible iodine-based contrast-enhanced computed tomography (DiceCT): An emerging tool for rapid, high-resolution, 3D imaging of metazoan soft tissues. *Journal of Anatomy*, *228*(6), 889–909.

Grosse, I. R., Dumont, E. R., Coletta, C., & Tolleson, A. (2007). Techniques for modeling muscle-induced forces in finite element models of skeletal structure. *The Anatomical Record*, *290*, 1069–1088.

Hedrick, B. P., Yohe, L., Linden, A. V., Dávalos, L. M., Sears, K., Sadier, A., Rossiter, S. J., Davies, K. T. J., & Dumont, E. (2018). Assessing soft-tissue shrinkage estimates in museum specimens imaged with diffusible iodine-based contrast-enhanced computed tomography (diceCT). *Microscopy and Microanalysis*, *24*, 284–291.

Holliday, C. M., & Witmer, L. M. (2007). Archosaur adductor chamber evolution: Integration of musculoskeletal and topological criteria in jaw muscle homology. *Journal of Morphology*, *268*, 457–484.

Holliday, C. M., & Witmer, L. M. (2009). The epipterygoid of crocodyliforms and its significance in the evolution of the orbitotemporal region of eusuchians. *Journal of Vertebrate Paleontology*, *29*(3), 713–733.

Holliday, C. M., & Gardner, N. M. (2012). A new eusuchian crocodilian with novel cranial integument and the origin of Crocodylia. *PLoS One*, *7*(1), e30471.

Holliday, C. M., Tsai, H. P., George, I. D., Skiljan, R. J., & Pathan, S. (2013). 3D integrative atlas of the jaw muscles of *Alligator mississippiensis*. *PLoS One*, *8*, e62806. https://doi.org/10.1371/journal.pone.0062806

Holliday, C. M., Porter, W. R., Vliet, K. A., & Witmer, L. M. (2019). The frontoparietal fossa of archosaurs and its significance for vascular and muscular anatomy. *The Anatomical Record*, *303*(4), 1060–1074.

Iordansky, N. N. (1964). The jaw muscles of the crocodiles and some relating structures of the crocodilian skull. *Anatomischer Anzeiger*, *115*, 256–280.

Jeffery, N., Stephenson, R. S., Gallagher, J. A., Jarvis, J. C., & Cox, P. G. (2011). Micro-computed tomography with iodine staining resolves the arrangement of muscle fibres. *Journal of Biomechanics*, *44*, 189–192.

Katzke, J., Puchenkov, P., Stark, H., & Economo, E. P. (2022). A roadmap to reconstructing muscle architecture from CT data. *Integrative Organismal Biology*, *4*(1), obac001.

Kerfoot, J. R., Fern, M. P., & Elsey, R. M. (2014). Scaling the feeding mechanism of captive *Alligator mississippiensis* from hatchling to juvenile. *Biology*, *3*(4), doi 10.3390/biology3040724–doi 10.3390/biology3040738.

Khalife, A., Keller, R. A., Billen, J., Garcia, F. H., Economo, E. P., & Peeters, C. (2018). Skeletomuscular adaptations of head and legs of *Melissotarsus* ants for tunnelling through living wood. *Frontiers Zool*, *15*(30), 30. https://doi.org/10.1186/s12983-018-0277-6

Klembara, J. (2004). Ontogeny of the palatoquadrate and adjacent lateral cranial wall of the endocranium in prehatching *Alligator mississippiensis* (Archosauria: Crocodylia). *Journal of Morphology*, *263*, 644–658.

Kupczik, K., Stark, H., Mundry, R., Neininger, F. T., Heidlauf, T., & Röhrle, O. (2015). Reconstruction of muscle fascicle architecture from iodine-enhanced microCT images: A combined texture mapping and streamline approach. *Journal of Theoretical Biology*, *382*, 34–43.

Kuzmin, I. T., Boitsova, E. A., Gombolevskiy, V. A., Mazur, E. V., Morozov, S. P., Sennikov, A. G., Skutchas, P. P., & Sues, H.-D.

(2021). Braincase anatomy of extant Crocodylia, with new insights into the development and evolution of the neurocranium in crocodylomorphs. *Journal of Anatomy*, *239*(5), 983–1038.

Lautenschlager S. 2013. Cranial myology and bite force performance of *Erlikosaurus andrewsi*: A novel approach for digital muscle reconstructions. *Journal of Anatomy 222*(2): 260–272.

Lautenschlager, S., Bright, J. A., & Rayfield, E. J. (2014). Digital dissection–using contrast-enhanced computed tomography scanning to elucidate hard-and soft-tissue anatomy in the common buzzard *Buteo*. *Journal of Anatomy*, *224*(4), 412–431.

Lautenschlager, S., Gill, P., Luo, Z.-X., Fagan, M. J., & Rayfield, E. J. (2017). Morphological evolution of the mammalian jaw adductor complex. *Biological Reviews*, *92*(4), 1910–1940.

Lessner, E. J. (2020). Quantifying neurovascular canal branching patterns reveals a shared crocodylian arrangement. *Journal of Morphology*, *282*, 185–204.

Lessner, E. J., & Holliday, C. M. (2020). A 3D ontogenetic atlas of *Alligator mississippiensis* cranial nerves and their significance for comparative neurology of reptiles. *The Anatomical Record*, 1-29. https://doi.org/10.1002/ar.24550

Li, Z., Clarke, J. A., Ketcham, R. A., Colbert, M. W., & Yan, W. (2015). An investigation of the efficacy and mechanism of contrast-enhanced X-ray computed tomography utilizing iodine for large specimens through experimental and simulation approaches. *BMC Physiology*, *15*, 5.

McHenry, C. R., Clausen, P. D., Daniel, W. J. T., Meers, M. B., & Pendharkar, A. (2006). Biomechanics of the rostrum in crocodilians: A comparative analysis using finite-element modeling. *The Anatomical Record*, *288*, 827–849.

Melstrom, K. M., & Irmis, R. B. (2019). Repeated evolution of herbivorous crocodyliforms during the age of dinosaurs. *Current Biology*, *29*(14), P2389–P2395.

Metscher, B. D. (2009). Micro-CT for comparative morphology: Simple staining methods allow high-contrast 3D imaging of diverse non-mineralized animal tissues. *BMC Physiology*, *9*(11), 1–14.

Morris, Z. S., Vliet, K. A., Abzhanov, A., & Pierce, S. E. (2021). Developmental origins of the crocodylian skull table and platyrostral face. *The Anatomical Record*, 1-29. https://doi.org/10.1002/ar.24802

Porro, L. B., Holliday, C. M., Anapol, F., Ontiveros, L. C., Ontiveros, L. T., & Ross, C. F. (2011). Free body analysis, beam mechanics, and finite element modeling of the mandible of Alligator mississippiensis. *Journal of Morphology*, *272*(8), 910–937.

Porro, L. B., Metzger, K. A., Iriarte-Diaz, J., & Ross, C. F. (2013). In vivo bone strain and finite element modeling of the mandible of *Alligator mississippiensis*. *Journal of Anatomy*, *223*(2), 195–227.

Schumacher, G. H. (1973). The head muscles and hyolaryngeal skeleton of turtles and crocodilians. In C. Gans & T. S. Parsons (Eds.), *Biology of the Reptilia. Vol. 4. Morphology D* (pp. 101–200). Academic Press.

Sellers, K. C., Davis, J. L., Middleton, K. M., & Holliday, C. M. (2017). Ontogeny of bite force in a validated biomechanical model of the American alligator. *Journal of Experimental Biology*, *220*(11), 2036–2046.

Sellers, K. C., Schmiegelow, B. A., & Holliday, C. M. (2019). The significance of enamel thickness in the teeth of *Alligator mississippiensis* and its diversity among crocodyliforms. *Journal of Zoology.*, *309*(3), 172–181.

Sellers KC. 2021. Function and evolution of the crocodyliform feeding apparatus. University of Missouri Dissertation. 157 pp.

Sellers KC, Nieto MN, Degrange FJ, Pol D, Clark JM, Middleton KM, and Holliday CM. 2022. The effects of skull flattening on Suchian jaw muscle evolution. *The Anatomical Record*, 1-32. https://doi.org/10.1002/ar.24912

Sullivan, S., McGechie, F. R., Middleton, K. M., & Holliday, C. M. (2019). 3D muscle architecture of the pectoral muscles of European Starling (*Sturnus vulgaris*). *Integrative Organismal Biology*, *1*, 1-18. https://doi.org/10.1093/iob/oby010

Tsai, H. P., & Holliday, C. M. (2011). Ontogeny of the cartilago transiliens of *Alligator mississippiensis* and its significance for sauropsid jaw muscle homology and sesamoid biology. *PLoS One*, *6*(9), e24935.

Tsai, H. P., & Holliday, C. M. (2016). Articular soft tissue anatomy of the archosaur hip joint: Structural homology and functional implications. *Journal of Morphology*, *276*, 601–630.

Vickerton, P., Jarvis, J., & Jeffery, N. (2013). Concentration-dependent specimen shrinkage in iodine-enhanced microCT. *Journal of Anatomy*, *223*, 185–193.

Weigl, R. (2014). Longevity of crocodilians in captivity. *International Zoo News*, *61*(5), 363–373.

Wilken, A. T., Middleton, K. M., Sellers, K. C., Cost, I. N., & Holliday, C. M. (2019). The role of protractor musculature in *Varanus exanthematicus* and its significance for cranial biomechanics. *Journal of Experimental Biology*, *222*(jeb201459), 1-14. https://doi.org/10.1242/jeb.201459

Wilken, A. T., Sellers, K. C., Cost, I. N., Rozin, R. E., Middleton, K. M., & Holliday, C. M. (2020). Connecting the chondrocranium: Biomechanics of the suspensorium in reptiles. *Vertebrate Zoology*, *70*(3), 275–290.

Wong, M. D., Spring, S., & Henkelman, R. M. (2013). Structural stabilization of tissue for embryo phenotyping using micro-CT with iodine staining. *PLoS One*, *8*, e84321. https://doi.org/10.1371/journal.pone.0084321

How to cite this article: Holliday, C. M., Sellers, K. C., Lessner, E. J., Middleton, K. M., Cranor, C., Verhulst, C. D., Lautenschlager, S., Bader, K., Brown, M. A., & Colbert, M. W. (2022). New frontiers in imaging, anatomy, and mechanics of crocodylian jaw muscles. *The Anatomical Record*, 1–15. https://doi.org/10.1002/ar.25011